Jia-Yush Yen
Associate Professor.

Chih-Jung Huang
Graduate Student.

Shu-Shung Lu
Professor.

Department of Mechanical Engineering,
National Taiwan University, Taipei, Taiwan

Stability of PDF Controller With Stick-Slip Friction Device

This paper presents the precision control of drive devices with significant stick-slip friction. The controller design follows the Pseudo-Derivative Feedback (PDF) control algorithm. Using the second order system model, the PDF controller offers arbitrary pole placement. In this paper, the stability proof for the controller with stick-slip friction is presented. On the basis of this proof, the stability criteria are derived. The paper also includes both the computer simulation and the experimental works to confirm the theoretical result. The experiments conducted on a Traction Type Drive Device (TTDD) shows that control accuracy of as high as ±1 arc − second is achieved.

1 Introduction

Stick-slip friction is a commonly encountered phenomenon in mechanical systems. As described in [2, 4, 10, 12, 17], stick-slip friction is the dominating factor that limits the performance of servo systems, and as stated in [17], this phenomenon has been the focus of many research efforts. During the past decade, many good results have been made available in the literature [1], . . . , [26].

The control of friction system is interesting not only because of its increased importance in the manufacturing industry but also because of the highly nonlinear nature that makes it very difficult to be characterized. Actually, more than half of the works are concerning either the modeling of the friction phenomenon or the identification of friction parameters [2, 4, 7, 9, 10, 12, 13, 14, 15, 18, 25]. Some of these works presented very detailed observations on the friction force behavior; however, they are usually quite limited results due to the highly dependent nature of the friction phenomenon. Among the more popular works, the Bristle model of Haessig [18] captures the most detailed physical phenomenon, but is relatively numerically inefficient. The reset integrator model of Haessig and Karnopp [25] does not capture as much details, but is numerically more efficient.

The research efforts on active friction compensation are mainly available in the Robotic area [4, 6, 8, 20, 23]. Some of the research interests are also directed toward the machine tool applications [2, 12, 15]. The research interests then proceeds to the study of the direction compensation of the friction effect [1, 5, 10, 11, 17, 19, 22]. In most cases, the friction force are modeled as a constant disturbance. The control strategy is basically canceling the disturbance force. The theoretical analysis becomes easy by assuming the friction disturbance is canceled a-priori. Another very common approach is to use a dither type excitation to eliminate the friction effect [8]. Their work covers mainly the experimental results. The development on active control involving stick-slip friction is more recent. Yang et al. [22] provided an adaptive version of the pulse width control. Theoretical analysis is also included. Since the parameters in the stick-slip friction model vary with many factors including load changes, lubrication conditions, and ambient temperatures, . . . , etc., many people apply adaptive techniques to the control problem [24, 16, 3, 22, 9]. The adaptive techniques are very effective at compensating for the slow varying friction force. It is also known to be sensitive to model structure mismatch. For low velocity friction compensation, the stick-slip friction becomes dominating. In this case more complicated control algorithms such as sliding mode controller [11], or two-degree-of-freedom controller [5] must be used. Analytical works on the direct stick-slip friction compensation is very involved. Few studies are available. Tung et al. in [5] mainly offered experimental results. [11] and [17] offered more theoretical results. Southward, et al. [17] offered a stability analysis using a cleaver Lyapunov function. Guzzella and Glattfelder [11] offered a stable controller using sliding mode approach. Both works based on the cancellation of the non-linear friction force.

In this paper, the authors observed that the friction system is intrinsically stable. Even though Southward [17] and Karnopp [25] had both pointed out that stick-slip friction often results in system instability. This instability arises only due to improper excitation. In other word, the authors would like to address the question on whether the simple control algorithms can achieve satisfactory control. In this paper, it is desirable to investigate the performance of the Pseudo Derivative Feedback (PDF) control for stick-slip friction drive. The PDF controller is used because it offers arbitrary pole placement for second-order systems. In addition, the PDF controller is capable of disturbance rejection from the input side. To achieve low speed friction compensation, this paper adopts the Karnopp stick-slip friction model. A Lyapunov function for the control system stability is presented. The limit set for the PDF control is derived. The experimental results show that the PDF controller achieves positioning accuracy better than ±1 arc − second.

2 Stick-Slip Friction Model

The servo-system under consideration contains a Traction Type Drive Device (TTDD) [28] with a servo motor as shown in Fig. 1. For the control purpose, the velocity response model is simplified by the commonly adopted first order system with stick-slip friction.

$$v_r = \dot{\theta}$$

$$\dot{v}_r + a v_r = (\tau - \tau_f) \tag{1}$$

where a is the system parameter, θ is the angular position, v_r is the angular velocity, τ is the applied input, and τ_f represents the friction effect.

The model for the stick-slip friction τ_f is introduced by Karnopp [25], and is shown in Fig. 2.

$$\tau_f = \tau_{\text{slip}}(v_r)[\lambda(v_r)] + \tau_{\text{stick}}(\tau)[1 - \lambda(v_r)] \tag{2}$$

Contributed by the Dynamic Systems and Control Divison for publication in the JOURNAL OF DYNAMIC SYSTEMS, MEASUREMENT, AND CONTROL. Manuscript received by the DSCD September 20, 1994. Associate Technical Editor: Tsu-Chin Tsao.

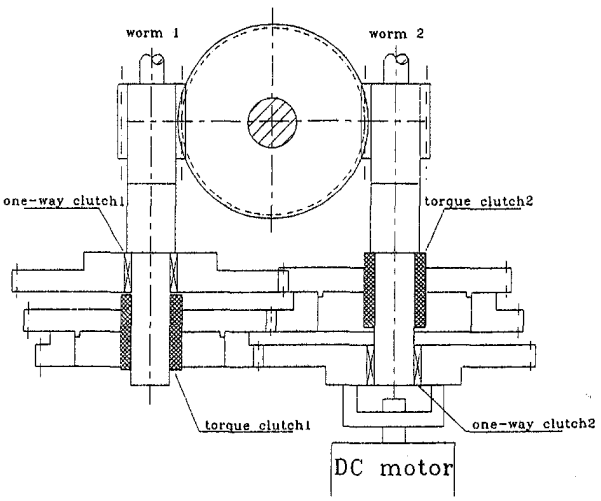

Fig. 1 Traction Type Drive Device (TTDD)

In (2),

$$\lambda(v_r) = \begin{cases} 1, & \text{for} \quad |v_r| > \sigma \\ 0, & \text{for} \quad |v_r| \le \sigma \end{cases} \qquad \sigma > 0. \tag{3}$$

The stick friction is represented by

$$\tau_{\text{stick}}(\tau) = \begin{cases} \tau_h^+, & \text{for} \quad \tau \ge \tau_h^+ > 0 \\ \tau, & \text{for} \quad \tau_h^- < \tau < \tau_h^+, \\ \tau_h^-, & \text{for} \quad \tau \le \tau_h^- < 0 \end{cases} \tag{4}$$

where $\tau_{\text{stick}}(\tau)$ represents stick force of friction when $|v_r| \le \sigma$. The positive and negative limits of the stick force are given by τ_h^+ and τ_h^-. When $|v_r| \le \sigma$ and the magnitude of the applied force is not larger than the limits of the stick force, the friction is equal to the applied force. The magnitudes of τ_h^+ and τ_h^- in (4) are not presumed equal. The value of σ is set to a small positive number only in the simulation to insure that the numerical integration algorithms remain stable.

The slip friction is modeled by

$$\tau_{\text{slip}}(v_r) = \tau_d^+(v_r)U(v_r - \sigma) + \tau_d^-(v_r)U(-v_r - \sigma). \tag{5}$$

$U(.)$ in (5) is the step function. The function $\tau_d^+(v_r)$ is the slip friction for positive velocity, and the function $\tau_d^-(v_r)$ is the slip friction for negative velocity. The magnitudes of $\tau_d^+(v_r)$ and $\tau_d^-(v_r)$ are not presumed to be symmetric. Generally speaking, the magnitude of $\tau_d^+(v_r)$ is no greater than τ_h^+; the magnitude of $\tau_d^-(v_r)$ is no greater than τ_h^-. Here, assume that $\tau_h = \max(|\tau_h^+|, |\tau_h^-|) = |\tau_f|$.

Altogether, Eq. (2) is used in the numerical simulation of τ_f as well as in the stability analysis.

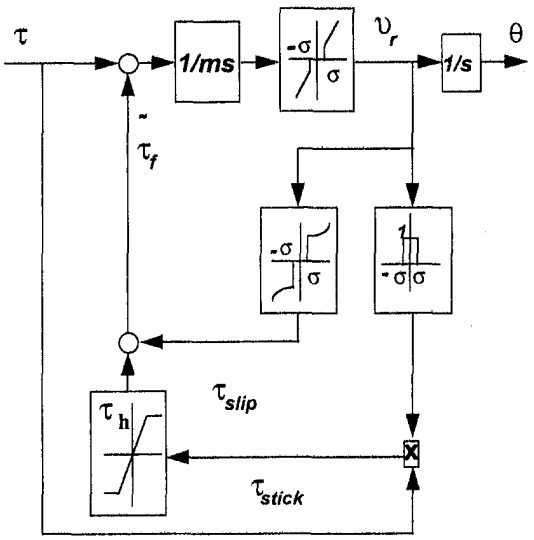

Fig. 2 Karnopp model

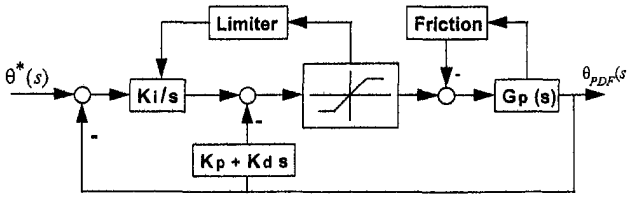

Fig. 3 PDF feedback control block diagram

3 Controller Design

Consider the PDF control block diagram in Fig. 3. Define the angular position $\theta = x_2$, the angular velocity $v = x_3$, and introduce an augmented state $x_1 = \int \theta dt$. If one set the reference input $\Theta^*(s)$ to be 0, it can be seen that PDF controller basically offers state feedback of the form

$$\underline{K} = [k_i \quad k_p \quad k_d]. \tag{6}$$

With some algebra, it can also be shown that this system is completely controllable. Arbitrary pole placement is possible.

Notice that the friction effect, τ_f, comes through a summing junction into the system input. Therefore, the friction force does not affect the close-loop poles. Using the PDF design technique to place the poles at $-r$, $-\alpha + \omega j$, and $-\alpha - \omega j$ where r, α and ω are positive reals. The resultant closed loop system becomes

$$\begin{aligned} \dot{x}_1 &= \int \theta dt \\ \dot{x}_2 &= \dot{x}_1 = \theta \\ \dot{x}_3 &= \dot{x}_2 = v_r \\ \dot{x}_3 &= -a_3 x_1 - a_2 x_2 - a_1 x_3 - \tau_f \end{aligned} \tag{7}$$

where

$$\begin{cases} a_1 = r + 2\alpha \\ a_2 = 2\alpha r + \alpha^2 + \omega^2 \\ a_3 = r(\alpha^2 + \omega^2) \end{cases} \tag{8}$$

The state space representation for the closed-loop system is thus

$$\begin{aligned} \dot{\underline{x}} &= \underline{A}\underline{x} + \underline{B}\tau_f \\ y &= \underline{C}\underline{x} \end{aligned} \tag{9}$$

where

$$\underline{x} = [x_1 \quad x_2 \quad x_3]',$$

$$\underline{A} = \begin{bmatrix} 0 & 1 & 0 \\ 0 & 0 & 1 \\ -a_3 & -a_2 & -a_1 \end{bmatrix}$$

$$\underline{B} = [0 \quad 0 \quad -1]'$$

$$\underline{C} = [0 \quad 1 \quad 0]$$

4 Stability Proof

Choose the following Lyapunov function candidate of the form.

$$V(\underline{x}) = \underline{x}'\underline{P}\underline{x} \tag{10}$$

and

$$\underline{P} = \begin{bmatrix} p_{11} & p_{12} & p_{13} \\ p_{12} & p_{22} & p_{23} \\ p_{13} & p_{23} & p_{33} \end{bmatrix} \tag{11}$$

where $\underline{P}$ is a real symmetric positive definite matrix.

From the well-known Lyapunov stability theorem, matrix $\underline{A}$ is a Hurwitz matrix, if and only if there exists some positive definite matrix $Q \in \Re^{n\times n}$, such that

$$\underline{A}'\underline{P} + \underline{P}\underline{A} = -\underline{Q} \tag{12}$$

has a corresponding unique solution for $\underline{P}$, and $\underline{P}$ is positive definite.

The derivative of $V(\underline{x})$ is given by

$$\begin{aligned} \dot{V}(\underline{x}) &= -\underline{x}'\underline{Q}\underline{x} - 2\underline{X}'\underline{P}\tau_f \\ &\le -\underline{\sigma}(\underline{Q})|\underline{x}|^2 + 2|\underline{x}\|\underline{PB}\|\tau_f| \\ &= -\underline{\sigma}(\underline{Q})|\underline{x}|(|\underline{x}| - (2|\underline{PB}|\tau_h)/\underline{\sigma}(\underline{Q})) \end{aligned}$$

Assume $x_r = 2|PB|\tau_h/\underline{\sigma}(\underline{Q})$ and $\delta > 0$, for all $|\underline{x}| > x_r + \delta$, than

$$\begin{aligned} \dot{V}(\underline{x}) &= -\underline{\sigma}(\underline{Q})|\underline{x}|(|\underline{x}| - x_r) \\ &\le -\underline{\sigma}(\underline{Q})|\underline{x}|\delta < 0 \end{aligned} \tag{13}$$

The system is bounded. The domain $B_r = \{\underline{x} \in \Re^3: |\underline{x}| \le x_r + \delta, \delta > 0\}$ is a positive limit set and an invariant set. Define the distance $d(p, \Omega)$ is the distance between a point p and a nonempty closed set Ω. For all initial condition $\underline{x}_0 \in \Re^3$, $t_0 \in \Re_+$ and trajectory $S(t, t_0, \underline{x}_0)$ of this system is satisfied that

$$d(S(t, t_0, \underline{x}_0), B_r) \to 0 \text{ as } t \to \infty.$$

And, given any $\epsilon > 0$ and $T < \infty$, there exists a $t - t_0 \ge T$ such that

$$d(S(t, t_0, \underline{x}_0), B_r) < \epsilon \tag{14}$$

From the above results, it satisfies the initial control specification that the state x_1 is bounded. In addition, the angular position state x_2 and the angular velocity state x_3 are also bounded.

From the above result, we can concentrate the focus on the final region for states x_2 and x_3. Consider the Lyapunov function candidate

$$\underline{Q} = \begin{bmatrix} 0 & 0 & 0 \\ 0 & q_{22} & q_{23} \\ 0 & q_{23} & q_{33} \end{bmatrix}, \tag{15}$$

where $q_{11} = q_{12} = q_{13} = q_{21} = q_{31} = 0$ means that the state x_1 is not considered. The solution of $\underline{P}$ is given by

$$\underline{P} = \begin{bmatrix} \dfrac{a_3^2 q_{33} + a_1 a_3 q_{22}}{2(a_1 a_2 - a_3)} & \dfrac{a_3(a_2 q_{33} + q_{22})}{2(a_1 a_2 - a_3)} & 0 \\ \dfrac{a_3(a_2 q_{33} + q_{22})}{2(a_1 a_2 - a_3)} & \dfrac{a_3(a_1 q_{33} - 2q_{23}) + a_2^2 q_{33} + a_2(q_{22} + 2a_1 q_{23}) + a_1^2 q_{22}}{2(a_1 a_2 - a_3)} & \dfrac{a_3 q_{33} + a_1 q_{22}}{2(a_1 a_2 - a_3)} \\ 0 & \dfrac{a_3 q_{33} + a_1 q_{22}}{2(a_1 a_2 - a_3)} & \dfrac{a_2 q_{33} + q_{22}}{2(a_1 a_2 - a_3)} \end{bmatrix}. \tag{16}$$

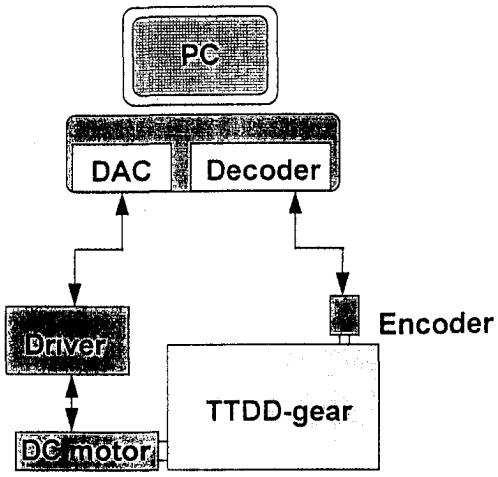

Fig. 4 Stick-slip friction experiment setup

It is straight forward to design the pole locations such that $\underline{P}$ is a positive definite matrix.

The derivative of $V(\underline{x})$ is

$$\dot{V}(\underline{x}) = -q_{22}x_2^2 + 2q_{23}x_2x_3 - q_{33}x_3^2 - 2p_{23}x_2\tau_f - p_{33}x_3\tau_f. \tag{17}$$

Let $q_{23} = \sqrt{q_{22}q_{33}} - \eta$, $\eta > 0$. After some algebra the limit set of x_2 and x_3 as $t \to \infty$ can be derived as

$$|x_2| \le \frac{a_3 q_{33} + a_1 q_{22}}{(a_1 a_2 - a_3)q_{22}}\tau_h + \delta_2 \quad \text{for some } \delta_2 > 0 \tag{18}$$

$$|x_3| \le \frac{(a_3 q_{33} + a_1 q_{22})^2 \tau_h}{4(a_1 a_2 a_3)(q_{22}^2 + a_2 q_{22} q_{33} + a_3\sqrt{q_{22}q_{33}^3} + a_1\sqrt{q_{22}^3 q_{33}})} + \delta_3 \quad \text{for some } \delta_3 > 0 \tag{19}$$

The positive parameters of q_{22} and q_{33} can be selected arbitrarily. Let $q_{22} = 1$ and $q_{33} \to \zeta$ for $\zeta > 0$. One can use Eq. (18) and Eq. (19) to obtain

$$|x_2| \le \frac{(r + 2\alpha)\tau_h}{2(\alpha(\alpha + r)^2 + \alpha\omega^2)} + \delta_2 \quad \text{for } \delta_2 > 0 \text{ as } t \to \infty \tag{20}$$

$$|x_3| \le \frac{(r + 2\alpha)^2 \tau_h}{8\alpha(2\alpha r + \alpha^2 + \omega^2 + r^2)} + \delta_3 \quad \text{for } \delta_3 > 0 \text{ as } t \to \infty \tag{21}$$

Referring to Eqs. (20) and (21), the larger the magnitudes of r, α and ω, the smaller the positive limit set for the position and the velocity. On the other hand, positioning accuracy can be improved by increasing r, α or ω. Notice that increasing ω produces high frequency input which is the same as using dither signals to remove the phenomena of stick-slip friction.

5 Experiment Setup

The experimental setup is shown in Fig. 4. The setup is based on a Traction Type Drive Device (TTDD). Conventional worm

gear drives with only one worm experience large backlash, but the TTDD with two worms eliminates the backlash effect and isolates the friction problem [28].

Referring to Fig. 1, when the worm wheel rotates in the counterclockwise direction, worm 1 drives the worm wheel and act as the load worm. The torque clutch on worm 2 will force worm 2 to retain on the worm wheel, and acts as the control worm. As the worm wheel reverses its rotation, worm 1 and worm 2 switch functions. Worm 2 becomes the load worm, and worm 1 becomes the control worm. The assistant mechanism accomplishes this switching. The detailed design specification for the TTDD can be found in [29].

The position measurement uses a Canon $K \cdot 1$ super high resolution encoder. The encoder produces 81,000 pulses/rev and achieves ± 1 arc − second resolution. The encoder measures the of worm wheel angle. A PC reads the pulses from the decoder and sends the voltage command through the DAC to the linear power amplifier that drives a Sanyo Denki U718T-012E DC servo motor.

6 Simulation and Experimental Results

Consider the control block diagram in Fig. 3. The identification is done by fitting the velocity response of the system into the ARMAX model in MATLAB. The resulted system transfer function is

$$G_p(s) = \frac{\Theta(s)}{V(s)} = \frac{1}{s(Is + a')}. \tag{22}$$

The parameters in (22) are $I = 6.652 \times 10^{-6}$ and $a' = 1.656 \times 10^{-5}$. The parameters in the Karnopp model, Fig. 2, are $\tau_h^+ = 0.78$ volt, the stick friction in the counterclockwise direction, $\tau_d^+ = 0.77$ volt, the slip friction in the counterclockwise direction, $\tau_h^- = 0.23$ volt, the stick friction in the clockwise direction, $\tau_d^- = 0.22$ volt, the slip friction in the clockwise direction, and zero-region σ in the Karnopp model equals 1×10^{-5}. These data are used for both the simulation and the controller design. For comparison purpose, the simulation and experimental results from PID controller will also be included.

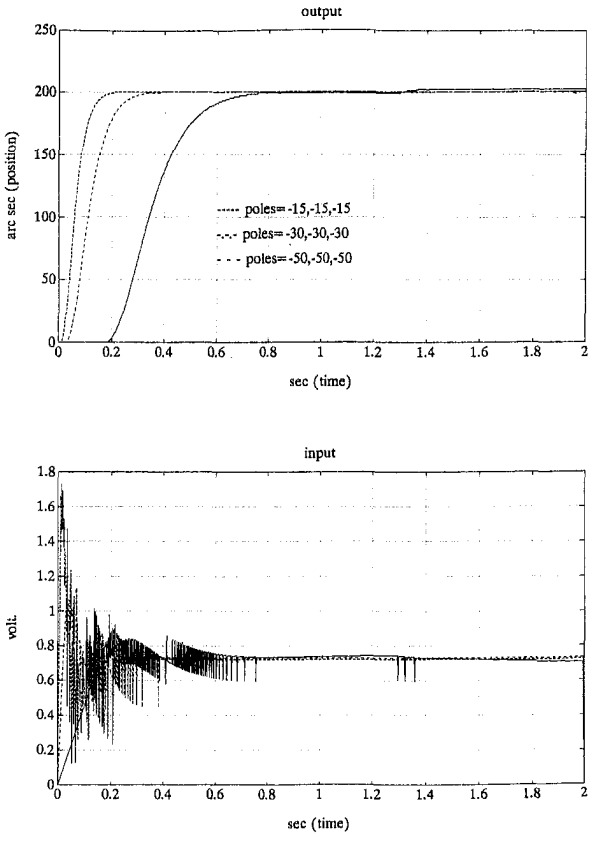

Fig. 5 Simulation results for PDF control on stick-slip friction system

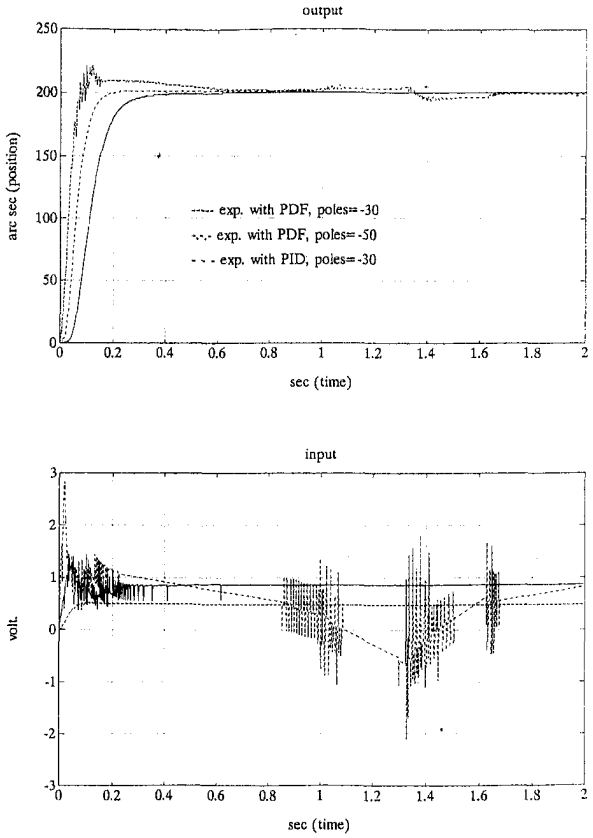

Fig. 6 Experiment results for PDF control on stick-slip friction system

The simulation results for the PDF control with various pole locations are shown in figure 5. Limit cycle exits when the gains are set too low (placing the poles at $p = -15$). This is in agreement with the theoretical analysis. Overshoot does not occur with the PDF control in Fig. 5. The poles can be placed arbitrarily far left in the s-plane for the PDF control, because the simulation program does not consider signal noises and drive saturation.

The experimental results with the PDF control is shown in Fig. 6. The results are the same as the simulation results for cases with poles placed at $p = -30$. Limit cycle appears again under the low gain situations ($p = -15$ for example). For properly tuned system, the distance traveled does not affect the control result. Figure 7 shows small distance steppings for step sizes of 2 seconds, 4 seconds, and 6 seconds. It can be seen that even with very small movement (2 seconds) the control can still achieve satisfactory control with no steady-state error.

7 Conclusions

This paper addressed the stability issue for the PDF control on the stick-slip friction system. The Karnopp model is used for the stick-slip friction force. The Lyapunov stability for the system is presented. The limiting set for the PDF control is also derived. The size of the limiting set can be designed with the PDF controller parameters. Therefore, it is possible to improve the control accuracy through careful controller design.

The experiment setup is based on the TTDD. The TTDD eliminates the backlash by using two worms combined with two one-way clutches and two torque clutches. The TTDD achieve

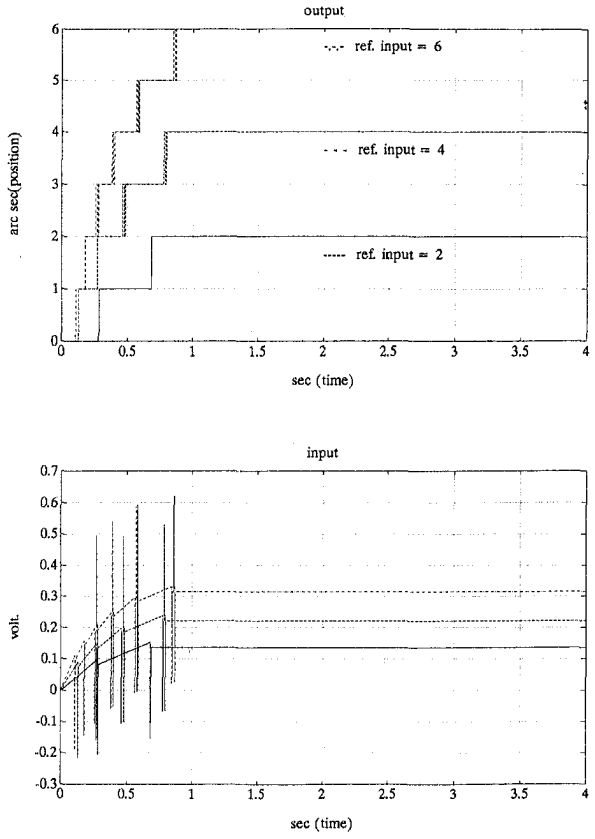

Fig. 7 Small steps PDF control on stick-slip friction system

backlashless and self-retaining operation. Both the simulation results and experimental results show very good agreement with the theoretical analysis. With proper tuning, the PDF controller achieves positioning accuracy to better than 1 arc-second.

Acknowledgments

This work is funded in part by a joint research project with the Giant Lion Know-How Co., Ltd., Taiwan, and in part by the National Science Council, R.O.C. under project No. NSC86-2212-E-002-049.

References

1 Newman, W. S., and Zhang, Y., 1994, "Stable interaction Control and Coulomb Friction Compensation Using Natural Admittance Control," *Journal of Robotics Systems,* Vol. 11, No. 1, pp. 3–11, 1994.

2 Cetinkunt, S., Yu, W. L., and Donmez, A., 1994, "Friction Characterization Experiments on a Single Point Diamond Turning Machine Tool," *Int. J. Mach. Tools Manufact,* Vol. 34, No. 1, pp. 19–32, 1994.

3 Canudas, C., 1993, "Robust Control for Servo-Mechanisms Under Inexact Friction Compensation," *Automatical,* Vol. 29, No. 3, pp. 757–761, 1993.

4 Phillips, Stephen M., and Ballou, Kevin R., 1993, "Friction Modeling and Compensation for an Industrial Robot," *Journal of Robotics Systems,* Vol. 10, No. 7, pp. 947–971, 1993.

5 Tung, E. D., and Tomizuka, M., 1993 "Feedforward Tracking Controller Design Based on the Identification of Low Frequency Dynamics," *Trans. ASME,* Vol. 115, Sept., 1993.

6 Feliu, Vicente, Rattan, K. S., and Brown, Jr, H. Benjamin, 1993, "Control of Flexible Arms with Friction in the Joints," *IEEE Transactions on Robotics and Automation,* Vol. 9, No. 4, August 1993 pp. 467–475.

7 Dohring, M. E., Lee, Eunjeong, and Newman, Wyatt S., 1993, "A Load-Dependent Transmission Friction Model: Theory and Experiments," *Proceedings of the IEEE Conference on Robotics and Automation,* pp. 430–437.

8 Yoshida, Yasuo. and Tanaka, Masato, 1993, "Position Control of a Flexible Arm Using a Dither Signal," *Jsme International Journal Series C,* Vol. 36, No. 1, 1993.

9 Yang, Y. P., and Chu, J. S., 1993, "Adaptive Velocity Control of Dc Motors With Coulomb Friction Identification," ASME JOURNAL OF DYNAMIC SYSTEMS, MEASUREMENT, AND CONTROL, Vol. 115, Mar. 1993, pp. 95–102.

10 Johnson, Craig T., and Lorenz, Robert D., 1992, "Experimental Identification of Friction and its Compensation in Precise, Position Controlled Mechanisms," *IEEE Transactions on Industry Applications,* Vol. 28, No. 6, Nov-Dec 1992 pp. 1392–1398.

11 Guzzella, L., and Glattfelder, A. H., 1992, "Positioning of Stick-Slip Systems-Comparison of a Conventional and a Variable-Structure Controller Design," *Proc. of 1992 ACC,* Wp13, pp. 1277–1281

12 Cetinkunt, C., Yu, W. L., Filliben, J., and Donmez, A., 1992 "Friction Characterization Experiments for Precision Machine Tool Control at Very Low Speeds," *Proc. of 1992 ACC,* WA11, pp. 404–408.

13 Hughes, R. O., 1992, "Effects of Friction on Precision Pointing Systems," *Proc. of 1992 ACC,* WA7, pp. 235–236

14 Bilman, P.-A. J., 1992, "Mathematical Study of the Dahl's Friction Model," *Eur, J. Mech.,* A/Solids, 11, No. 6, pp. 835–848, 1992

15 Tu, J. F., and Stein, J. L. 1992, "On-Line Preload Monitoring for Anti-Friction Spindle Bearings of High-Speed Machine Tools," *Proc. of 1992 ACC,* WA11, pp. 361–369

16 Friendland, B. and Park, Y. J., 1991 "On Adaptive Friction Compensation," *Proceedings of the IEEE Conference on Precision and Control.* Vol. 3, pp. 2899–2902.

17 Southward, S. C., Radcliffe, C. J. and MacCluer, C. T., 1991, "Robust Nonlinear Stick-Slip Friction Compensation," ASME JOURNAL OF DYNAMIC SYSTEMS, MEASUREMENT, AND CONTROL, Vol. 113, Dec. 1991, pp. 639–645.

18 Haessig, Jr. D. A. and Friedland, B., 1991, "On the Modeling and Simulation of Friction," ASME JOURNAL OF DYNAMIC SYSTEMS, MEASUREMENT, AND CONTROL, Vol. 113, Sept. 1991, pp. 354–362

19 Canudas, C., and Seront, V., 1990, "Robust Adaptive Friction Compensation," *IEEE International Conf. on Robotics and Automation,* U.S.A., pp. 1383–1388, 1990

20 Canudas, C., Noel, P., Aubin, A., Brogliato, P., and Drevet, P., 1989 "Adaptive Friction Compensation in Robot Manipulators: Low-Velocities" *IEEE International Conf. on Robotics and Automation,* Scottsdale, Arizona. U.S.A., pp. 1352–1357, 1989

21 Armstrong, B., 1988, "Friction: Experimental Determination, Modeling and Compensation," *Proceedings of the 1988 IEEE International Conference on Robotics and Automation,* Vol. 3, pp. 1422–1427

22 Yang, S., and Tomizuka, M., 1988, "Adaptive Pulse Width Control for Precise Positioning Under the Influence of Stiction and Coulomb Friction," ASME JOURNAL OF DYNAMIC SYSTEMS, MEASUREMENT, AND CONTROL, Vol. 110, Sept. 1988, pp. 221–227.

23 Kubo, T., Anwar, G., and Tomizuka, M., 1986, "Application of Nonlinear Friction Compensation to Robot Arm Control," *Proceedings of the 1986 IEEE International Conference on Robotics and Automation,* Vol. 2, pp. 722–727

24 Canudas, C., Astrom, K. J., and Braun, K., 1986, "Adaptive Friction Compensation in DC Motor Drives," *IEEE J. Rob. Auto.,* V.RA-3, n. 6, Dec 1987, pp. 681–685.

25 Karnopp, D., 1985, "Computer Simulation of Stick-Slip Friction in Mechanical Dynamic Systems," ASME JOURNAL OF DYNAMIC SYSTEMS, MEASUREMENT, AND CONTROL, Vol. 107, Mar. 1985 pp. 100–103.

26 Marui, Etsuo, and Kato, Shinobu, 1984, "Forced Vibration of a Base-Excited Single-Degree-of-Freedom System With Coulomb Friction," *Trans. ASME,* Vol. 106, Dec, 1984

27 Phelan, R. M., *Feedback Control System,* Cornell University Press, Ithaca, NY.

28 Yang, T. H., 1993, "Douple Acting Type Dynamic Back Spacing Removed Driving System," US patent No. 5265488.

29 Huang, C. J., Yen, J. Y., and Lu, S. S., 1994, "The combination of TTDD and PDF control for backlashless operation," ASME JOURNAL OF DYNAMIC SYSTEMS, MEASUREMENT, AND CONTROL, Submitted.